


Original Research

SRPK Inhibitors Reduce the Phosphorylation and Translocation of SR Protein Splicing Factors, thereby Correcting *BIN1*, *MCL-1* and *BCL2* Splicing Errors and Enabling Apoptosis of Cholangiocarcinoma Cells

Preenapan Changphasuk¹, Chaturong Inpad¹, Sukanya Horpaopan², Sasiprapa Khunchai³, Suchada Phimsen¹, Damratsamon Surangkul¹, Tavan Janvilisri⁴, Atit Silsirivanit⁵, Worasak Kaewkong^{1,*} 

¹Department of Biochemistry, Faculty of Medical Science, Naresuan University, 65000 Phitsanulok, Thailand

²Department of Anatomy, Faculty of Medicine, Chiang Mai University, 50200 Chiang Mai, Thailand

³Department of Anatomy, Faculty of Medical Science, Naresuan University, 65000 Phitsanulok, Thailand

⁴Department of Biochemistry, Faculty of Science, Mahidol University, 10400 Bangkok, Thailand

⁵Department of Biochemistry, Faculty of Medicine, Khon Kaen University, 4002 Khon Kaen, Thailand

*Correspondence: worasakk@nu.ac.th (Worasak Kaewkong)

Academic Editor: Kishu Ranjan

Submitted: 23 June 2024 Revised: 5 September 2024 Accepted: 12 September 2024 Published: 29 September 2024

Abstract

Background: Cholangiocarcinoma (CCA) is a malignancy of the bile duct epithelium that is commonly found in the Thai population. CCA has poor prognosis and a low survival rate due to the lack of early diagnosis methods and the limited effectiveness of current treatments. A number of oncogenic spliced-transcripts resulting from mRNA splicing errors have been reported in CCA, and aberrant mRNA splicing is suspected to be a key driver of this cancer type. The hyperphosphorylation of serine/arginine rich-splicing factors (SRSFs) by serine/arginine protein kinases (SRPKs) causes them to translocate to the nucleus where they facilitate gene splicing errors that generate cancer-related mRNA/protein isoforms. **Methods:** The correlation between SRPK expression and the survival of CCA patients was analyzed using data from The Cancer Genome Atlas (TCGA) dataset. The effect of SRPK inhibitors (SRPIN340 and SPHINX31) on two CCA cell lines (KKU-213A and TFK-1) was also investigated. The induction of cell death was studied by Calcein-AM/PI staining, AnnexinV/7AAD staining, immunofluorescence (IF), and Western blotting (WB). The phosphorylation and nuclear translocation of SRSFs was tracked by WB and IF, and the repair of splicing errors was examined by Reverse Transcription-Polymerase Chain Reaction (RT-PCR). **Results:** High levels of SRPK1 and SRPK2 transcripts, and in particular SRPK1, correlated with shorter survival in CCA patients. SRPIN340 and SPHINX31 increased the number of dead and apoptotic cells in a dose-dependent manner. CCA also showed diffuse expression of cytoplasmic cytochrome C and upregulation of cleaved caspase-3. Moreover, SRSFs showed low levels of phosphorylation, resulting in the accumulation of cytoplasmic SRSF1. To link these phenotypes with aberrant gene splicing, the apoptosis-associated genes Bridging Integrator 1 (*BIN1*), Myeloid cell leukemia factor 1 (*MCL-1*) and B-cell lymphoma 2 (*BCL2*) were selected for further investigation. Treatment with SRPIN340 and SPHINX31 decreased anti-apoptotic *BIN1+12A* and increased pro-apoptotic *MCL-1S* and *BCL-xS*. **Conclusions:** The SRPK inhibitors SRPIN340 and SPHINX31 can suppress the phosphorylation of SRSFs and their nuclear translocation, thereby producing *BIN1*, *MCL-1* and *BCL2* isoforms that favor apoptosis and facilitate CCA cell death.

Keywords: alternative splicing; apoptosis; cholangiocarcinoma; SRPK; SRSF

1. Introduction

Cholangiocarcinoma (CCA) is a severe type of cancer that arises from the uncontrolled growth of bile duct epithelium. CCA can be classified according to its anatomical origin into intrahepatic (iCCA) and extrahepatic (eCCA) types [1]. An increasing incidence of CCA has been reported globally, especially in the north and northeast regions of Thailand [2]. The main etiological factor is the consumption of undercooked freshwater fish contaminated with the infective stage of liver fluke, *Opisthorchis viverrini* (OV). The excretory/secretory products of OV contain important growth factors and growth stimuli. Other risk

factors for CCA are exogenous carcinogens that generate cellular DNA damage, and repeated treatment with anti-parasitic drugs [3,4]. Depending on the stage at diagnosis, CCA treatment strategies can include surgical resection, locoregional therapies, chemotherapy, and radiation therapy. Chemotherapy in combination with radiation has been shown to improve survival. The combination of Cisplatin and Gemcitabine is currently the first-line treatment for CCA [1]. However, most CCA patients are asymptomatic in the early stages of disease, thereby allowing tumor progression and metastasis to other organs. Consequently, the mortality rate for CCA patients has shown no significant improvement.



Aberrant alternative mRNA splicing in cancer cells results in the production of oncogenic isoforms of important genes and may be another hallmark of cancer [5]. The aberrant mRNA transcripts and their translatable proteins have unique properties that promote cell growth, differentiation and other cancer cell characteristics [6]. Several important oncogenic spliced genes have been reported in CCA. Cluster of differentiation 44 (*CD44*) produces *CD44v6*, which is related to tumor cell proliferation, and *CD44v8-10*, which is related to chemo-resistance. Wnt-Inducible Secreted Protein 1 (*WISP1*) produces *WISP1v*, which is related to migration-invasion ability, while Anterior Gradient-2 (*AGR2*) produces *AGH2vH* which is related to metastasis, epithelial-mesenchymal transition, and cell survival under stress [7,8]. Another example of dysregulated mRNA splicing is the switching from a wild-type transcript with pro-apoptotic function in normal cells into oncogenic transcripts with survival functions in cancer cells. Bridging Integrator 1 (*BINI*) is a tumor suppressor gene that functions by interacting with and inhibiting cellular myelocytomatosis oncogene (*c-MYC*). The inclusion of exon 12A of *BINI* generates a protein isoform that can no longer bind Myc, thus eliminating the tumor-suppressive function of BIN1 in melanoma, prostate and non-small cell lung cancer [9–11]. Myeloid cell leukemia factor 1 (*MCL-1*) is a member of the B-cell lymphoma 2 (*BCL-2*) family and splices into two opposite isoforms. The short isoform (*MCL-1S*) exhibits pro-apoptotic activity, whereas the long isoform (*MCL-1L*) functions as an anti-apoptotic factor in basal cell carcinoma, breast cancer and leukemia [12–14]. *BCL-2L1* is a member of the BCL-2 family and generates two isoforms. *BCL-xL* prevents apoptosis, while *BCL-xS* promotes apoptosis in lung cancer, melanoma and breast cancer [15–17].

Serine/arginine-rich splicing factors (SRSFs) in the SR protein family serve as key molecules in the splicing machinery. The 12 SRSF members, SRSF1 to SRSF12, have different binding targets on pre-mature mRNA sequences [18]. The activation of SRSFs occurs after phosphorylation of serine/arginine-rich domains by serine-arginine protein kinases (SRPKs). The phosphorylated SRSFs then translocate from the cytoplasm to the nucleus to splice their specific pre-mature mRNA [19]. Dysregulation of SRSFs and SRPKs can lead to abnormal protein synthesis due to overexpression or functional alteration, thus revealing the oncogenic properties of the synthesized protein isoforms. A previous study on extra-nodal NK/T-cell lymphoma cells found that two SRPK inhibitors (SPHINX31 and SRPIN340) and siRNA can induce lymphoma cell death by increasing apoptosis, as shown by higher levels of Poly-Adenosine diphosphate ribose polymerase (PARP) and caspase-3 cleavage products [20]. Moreover, treatment with SRPIN340 decreased the phosphorylated forms of SRSF4, SRSF6, SRSF5, and SRSF2 in the HL60 and Jurkat human leukemic cell lines [21]. A similar result was

also found after treatment of SPEC-2 endometrial cancer cells with SPHINX31. SRPK1 treatment reduced the level of phosphorylated SRSFs, which subsequently downregulated the survivin protein and increased PARP cleavage to enable SPEC-2 cell apoptosis [22]. The effect of SRPK inhibitors on specific SRSFs has previously been reported in a CCA cell line [23]. Treatment of HuCCA-1 cells with SPHINX31 decreased the phosphorylation and nuclear localization of SRSF1, which is the predominant SRSF in CCA.

The aim of this study was therefore to investigate the effects of two SRPK inhibitors (SRPIN340 and SPHINX31) on two CCA cell lines: KKU-213A, representing OV-associated iCCA, and TFK-1, representing non-OV associated eCCA. We evaluated the induction of cell death and apoptosis by these SRPK inhibitors. The effects of SRPK inhibitors on SRSF phosphorylation and on the nuclear translocation of SRSF1 protein were also investigated. Finally, splice gene variants for the apoptosis-related genes *BINI*, *MCL-1* and *BCL2* were investigated as downstream targets of isoform switching, wherein the pro-apoptotic isoforms promote CCA cell apoptosis.

2. Methods

2.1 Cell Lines and Cell Culture

The KKU-213A cell line was established from a 58-year-old male diagnosed with iCCA at the Srinagarind Hospital, Khon Kaen University, Thailand, which the patients' informed consent and the research protocol (HE621403) was formerly approved by the Ethics Committee for Human Research of Khon Kaen University [24]. KKU-213A is a highly invasive cell line and is OV-associated. TFK-1 was purchased from the cell bank of the RIKEN BioResource Research Center (BRC). This cell line was derived from a 63-year-old male with eCCA [25]. KKU-213A was cultured in Gibco™ Dulbecco's Modified Eagle Medium (DMEM) (Thermo Scientific, Waltham, MA, USA), while TFK-1 was cultured in Gibco™ Roswell Park Memorial Institute (RPMI) 1640 Medium (Thermo Scientific, Waltham, MA, USA). All media contained 10% (v/v) Gibco™ fetal bovine serum (FBS, Thermo Scientific, Waltham, MA, USA), 100 Unit/mL penicillin and 100 µg/mL streptomycin. Cells were cultured in a humidified incubator (Thermo Scientific, Waltham, MA, USA) at 37 °C with a 5% CO₂ atmosphere. The authenticity of the cell lines was validated using Short Tandem Repeat (STR) DNA profiling. All cell lines were free of mycoplasma and were periodically tested using the Mycoalert assay (Lonza, Rockland, ME, USA).

2.2 SRPK Inhibitors and Treatments

The two SRPK inhibitors, SRPIN340 and SPHINX31, were purchased from Cayman chemical (Cayman Chemical Company, Ann Arbor, MI, USA). Both were dissolved in dimethyl sulfoxide (DMSO) (Merck KGaA, Darmstadt,

Germany) and stored at 4 °C. Cells were treated with various concentration of SRPK inhibitors (10 and 20 µM) for 18 h, with 0.5% (v/v) DMSO used as the vehicle control (0 µM of SRPK inhibitors).

2.3 TCGA Dataset Analysis

The on-web analytic tool Gene Expression Profiling Interactive Analysis (GEPIA) based on The Cancer Genome Atlas (TCGA) and the Genotype-Tissue Expression (GTEx) datasets (<http://gepia.cancer-pku.cn/>) was used for survival analysis of *SRPK1* and *SRPK2* expression in CCA. Cholangiocarcinoma is abbreviated as CHOL in GEPIA, while liver hepatocellular carcinoma is abbreviated as LIHC. The number of CHOL samples in the dataset is 36 tumor tissues and 9 normal tissues, while the number of LIHC samples is 369 tumor tissues and 160 normal tissues. Box-plot analysis was used to illustrate differences in *SRPK1* and *SRPK2* expression (transcripts per million, TPM) between tumor (T) and normal (N) tissues. The relationship between *SRPK1* or *SRPK2* expression and the overall survival of CHOL patients was also analysed.

2.4 Dual Staining for Live/Dead Cells

Cells were cultured in 96-well plates (1.6×10^4 cells per well) for 24 h to reach confluency of adhered cells. After treatment with SRPK inhibitors (0, 10 or 20 µM) for 18 h, the cells were stained and analyzed using the Live/Dead double staining kit (Merck KGaA, Darmstadt, Germany). The cells were first centrifuged at 1500 rpm for 5 min at 25 °C. A 50 µL aliquot of buffer (1 µL of 1 µM Cytochrome c, 1 µL of 1 mg/mL propidium iodide, and 1000 µL of staining buffer) was then added, followed by incubation at 37 °C for 15 min. Fluorescently stained cells were subsequently examined under a fluorescence microscope (Zeiss, Oberkochen, Germany) and the number of dead cells (red fluorescent stain) counted.

2.5 Flow Cytometry with AnnexinV/7-AAD Staining

Cells were cultured in a 24-well plate (1×10^5 cells per well) for 24 h and then treated with SRPK inhibitors (0, 10 or 20 µM) for 18 h. An equal volume of cell suspension (5×10^4 cells) was mixed with 75 µL of MUSE™ AnnexinV and Death Cell Reagent (Cytek Biosciences, Fremont, CA, USA). After 20 min incubation at room temperature in the dark, the cells were injected into capillary flow cells. For analysis, the cells (events) were gated, counted and subsequently collected into four quadrants with positive or negative AnnexinV and positive or negative 7-AAD. The proportions of live cells, dead cells and apoptotic cells (early and late stages) were analyzed as the percentage of total events using the Muse® Cell Analyzer and attached analytical software (Merck KGaA, Darmstadt, Germany).

2.6 Immunofluorescence (IF)

Cells were cultured (5×10^4 cells per chamber) in an 8-well cell culture slide for 24 h and then treated with SRPK inhibitors (0, 10 or 20 µM) for 18 h. They were subsequently fixed with 4% (v/v) paraformaldehyde (Merck KGaA, Darmstadt, Germany) for 30 min at room temperature, permeabilized with 0.2% (v/v) Triton-X (Merck KGaA, Darmstadt, Germany) for 5 min, and non-specific binding was blocked by incubation with 1:20 FBS for 20 min. The cells were then incubated overnight at 4 °C with the following primary antibodies: 1:100 rabbit anti-human Cytochrome C (Cell signaling Technology, Danvers, MA, USA), and 1:1000 mouse anti-human SRSF1 (Thermo scientific, Waltham, MA, USA). This was followed by incubation with the respective secondary antibodies: 1:100 goat anti-rabbit IgG-FITC (Merck KGaA, Darmstadt, Germany), or 1:100 goat anti-mouse IgG-Cy3 (Merck KGaA, Darmstadt, Germany). The cells were then counter stained with a 1:10,000 dilution of 4',6-diamidino-2-phenylindole (DAPI) (Merck Millipore, MA, USA) to stain the cell nuclei, and examined under a fluorescence microscope (Zeiss, Oberkochen, Germany).

2.7 Protein Extraction and Fractionation

For the extraction of whole cell lysate proteins, total cells from each treatment group were lysed in radio-immunoprecipitation (RIPA) buffer (Thermo scientific, Waltham, MA, USA) containing phosphatase inhibitor (Merck KGaA, Darmstadt, Germany) and protease inhibitor (Thermo scientific, Waltham, MA, USA). For protein fractionation, cells were lysed in Buffer A (10 mM HEPES KOH pH 7.9, 1.5 mM MgCl₂, 10 mM KCl, 0.1% NP-40, 0.5 mM DTT) and centrifuged at 5000 rpm for 1 min at 4 °C to collect cytoplasmic proteins in the supernatant. The pellets were subsequently extracted with Buffer B (50 mM HEPES KOH pH 7.9, 10% glycerol, 420 mM NaCl, 5 mM MgCl₂, 10 mM KCl, 0.1 mM EDTA, 1 mM DTT), sonicated, and then centrifuged at 15,000 rpm for 15 min, at 4 °C to collect nuclear proteins in the supernatant [26]. The Bradford assay was used to measure the protein concentration of extracted or fractionated samples. Bradford solution (Bio-Rad laboratories, Hercules, CA, USA) (200 µL) was mixed with 1 µL of protein sample (10-fold dilution), or with increasing concentrations (0, 0.1, 0.2, 0.3, 0.4, and 0.5 mg/mL) of bovine serum albumin (BSA; Capricorn scientific, Ebsdorfergrund, Germany) used as a standard. Absorbance was measured at 595 nm to calculate the protein concentration.

2.8 Sodium Dodecyl Sulfate-Polyacrylamide Gel Electrophoresis (SDS-PAGE) and Western Blotting

Equal amounts of protein from each treatment group were separated using SDS-PAGE (5% stacking gel and 12–15% separating gel), transferred to PVDF membrane (Bio-Rad laboratories, Hercules, CA, USA), and blocked us-

ing 5% BSA (Capricorn scientific, Ebsdorfergrund, Germany). The PVDF membranes were incubated overnight at 4 °C with the following primary antibodies: 1:1000 rabbit anti-human cleaved caspase-3 (Cell signaling Technology, Danvers, MA, USA), 1:10,000 rabbit anti-human GAPDH (Merck KGaA, Darmstadt, Germany), 1:1000 mouse anti-phosphoepitope SR protein (Merck KGaA, Darmstadt, Germany), 1:1000 rabbit anti-human beta-actin (Cell signaling Technology, Danvers, MA, USA), 1:10,000 mouse anti-human SRSF1 (Thermo scientific, Waltham, MA, USA), or 1:1000 rabbit anti-human Lamin B1 (Cell signaling Technology, Danvers, MA, USA). They were subsequently probed with HRP-conjugated goat anti-mouse IgG (Merck KGaA, Darmstadt, Germany), or HRP-conjugated goat anti-rabbit IgG (Merck KGaA, Darmstadt, Germany) for 1 h. Protein bands were detected using the enhanced chemiluminescence (ECL) detection system (Bio-Rad laboratories, USA) and imaged by ImageQuant™ LAS 500 (GE Healthcare Life Science, Amersham, UK). The immobilon® ECL ultra-western HRP substrate (Merck KGaA, Darmstadt, Germany) was used to enhance the signal strength of nuclear fractionated proteins samples. The signal intensity of each band was quantified using Image J software (Version 1.54, National Institutes of Health (NIH)'s Center for Information Technology, Bethesda, MD, USA) and the PVDF membranes were imaged using the Amersham ImageQuant™ 800 biomolecular imager (Cytiva, Amersham, UK). Lastly, the signal intensity of each band was quantified by ImageJ software and normalized to GAPDH, beta-actin or Lamin B1 protein expression.

2.9 RNA Extraction, cDNA Synthesis and Reverse Transcription-Polymerase Chain Reaction (RT-PCR)

RNA samples were isolated from harvested cells in each treatment group using the E.Z.N.A.® Total RNA Kit 1 (Omega Bio-Tek, Inc., Norcross, GA, USA). The RNA concentration was measured by NanoDrop 2000 (Thermo scientific Wilmington, DE, USA) and 1 µg was used to synthesize complementary DNA (cDNA) with the iScript™ Reverse Transcription Supermix (Bio-Rad Laboratories, Hercules, CA, USA) according to the manufacturer's instructions. Quantitative PCR was performed to determine the mRNA expression level of target genes. Reaction mixtures (20 µL) were prepared using 200 ng cDNA, 0.4 µM of each of the forward and reverse primers, and 1X MyTaq™ HS Red Mix (Bioline Reagents Limited, London, UK). Sequences for the PCR primers of each target gene are shown in Table 1. Thermocycling conditions consisted of 5 min pre-denaturation at 95 °C, 40 cycles of 95 °C for 30 sec, 62 °C for 30 sec and 72 °C for 30 sec for cycling amplification, and 72 °C for 5 min for final extension. PCR amplification products were mixed with 6× fluorescent DNA staining reagent (Novel Juice, Gene DireX, Taoyuan, Taiwan) and analysed by 3% agarose gel electrophoresis. Band intensities were evaluated by Amersham ImageQuant™ LAS500

(GE Healthcare Life Science, Amersham, UK) and quantitated using Image J software, with beta-actin used for semi-quantitative normalization.

2.10 Statistical Analysis

Data were presented as the mean ± standard deviation (SD) of triple biological replicates. The statistical significance of differences between two groups was determined with the Student's *t*-test, with *p* < 0.05 considered to indicate statistical significance.

3. Results

3.1 Expression of SRPK1 and SRPK2 in CCA from the TCGA Dataset, and Correlation with Survival

Intrahepatic CCA is a malignant epithelial neoplasm characterized by biliary differentiation within the liver. The anatomical origins of intrahepatic CCA overlap with those of liver cancer, thus limiting the application of differential screening by ultrasound and Computed Tomographic scan. Furthermore, the cancer registry database of the National Cancer Institute of Thailand reports that combined liver and bile duct cancer is the most common cancer type in the Thai population. The expression level (TPM counts) of *SRPK1* and *SRPK2* in tumor (T) and normal adjacent (N) tissues from the TCGA databases were compared using the GEPIA on-line web tool. In CHOL, both *SRPK1* and *SRPK2* expression were significantly higher in T compared to N tissue (Fig. 1A). In LIHC, the average expression of both *SRPK1* and *SRPK2* was higher in T compared to N tissues, but the difference was not statistically significant (Fig. 1B). The correlation of gene expression with the overall survival of CHOL patients was also analyzed. High *SRPK1* expression was associated with shorter overall survival (50% survival after 10–15 months vs. 40 months for low expression), with a hazard ratio for death of 2.3 (Fig. 1C). High *SRPK2* expression was not significantly related to overall survival (Fig. 1D).

3.2 Effect of SRPK Inhibitors on the Induction of CCA Cell Death

We next studied the effect of SRPK inhibitors on the induction of CCA cell death. The differential live/dead cell count was monitored by dual staining. In viable cells, the esterase enzyme catalyzes calcein into calcein-am, which emits green fluorescence. Moreover, PI passes through the nuclear membrane and binds to the DNA of dead cells, emitting red fluorescence. In both KKKU-213A (Fig. 2A) and TFK-1 (Fig. 2B) cells, the confluence of stained viable cells decreased following treatment with SRPK inhibitors (as observed by fluorescence microscopy, 20× and 40×), whereas the number of red fluorescent cells increased compared to the vehicle control. Both SRPK inhibitors caused a dose-dependent increase in the number of dead KKKU-213A cells, especially SPHINX31 which induced cell death even at 10 µM (Fig. 2C). For TFK-1 cells, the number of

Table 1. Sequences of the specific primers used in this study.

Primer name	Sequence (5' to 3')	bases	product size (bp)
<i>BIN1_All</i>	Forward: TGA TGT GGT GCT GGT GAT CC	20	311
	Reverse: GAC CTA ATC TTT GGG AGA ACG CC	23	
<i>BIN+I2A</i>	Forward: GGC CCA GCC CAG AAA GAA AAG TA	23	214
	Reverse: GCC TTT CCG GAG CTG AGA TGG G	22	
<i>MCL-1L</i>	Forward: GGA CAC AAA GCC AAT GGG CAG GT	23	426
<i>MCL-1S</i>	Reverse: GCA AAA GCC AGC AGC ACA TTC CTG A	25	178
<i>BCL-xL</i>	Forward: AGT AAA GCA AGC GCT GAG GGA G	22	439
<i>BCL-xS</i>	Reverse: ACT GAA GAG TGA GCC CAG CAG A	22	250
<i>Beta-actin</i>	Forward: AGT CGG TTG GAG CGA GCA TC	20	295
	Reverse: GGG CAC GAA GGC TCA TCA TT	20	

BIN1, Bridging Integrator 1; *MCL-1*, Myeloid cell leukemia factor 1; *BCL*, B-cell lymphoma.

red fluorescent cells increased significantly in all treatment groups, but the dose-dependent effect was observed only with SPHINX31 treatment (Fig. 2D).

3.3 Effect of SRPK Inhibitors on CCA Cell Apoptosis

The dead cell phenotype of CCA cells following treatment with SRPK inhibitors was investigated by flow cytometry after AnnexinV/7-AAD staining. Treated cells were stained and classified into four staining quadrants. High annexinV staining but low 7-AAD staining was gated as early apoptosis, whereas positive staining for both annexinV and 7-AAD was gated as late-stage apoptosis. For KKU-213A, an increasing number of early apoptotic cells was observed after treatment with the SRPK inhibitors, especially with 20 μ M SPHINX31 (Fig. 3A). For TFK-1, dose-dependent effects were observed with both SRPIN340 and SPHINX31, with a >50% apoptotic cell population observed after treatment with 20 μ M SPHINX31 (Fig. 3B).

3.4 Effect of SRPK Inhibitors on the Activation of Apoptosis-related Proteins in CCA Cells

Cytochrome C is a mitochondrial protein that is released into the cytosol to form the apoptosome, which subsequently activates caspase enzymes. IF and confocal microscopy were used here to assess the intracellular diffusion of cytochrome C, with green fluorescence representing the localization of cytochrome C and merging with DAPI to mark the nuclei. Untreated controls revealed perinuclear staining with cytoplasmic spots (granular pattern) representing cytochrome C localized in the mitochondria. Following treatment with SRPIN340 or SPHINX31, a diffuse cytoplasmic staining pattern was observed for cytochrome C in KKU-213A (Fig. 3C) and TFK-1 (Fig. 3D) cells. Moreover, lower confluencies were observed for the treated cells in a dose-dependent-manner.

Caspase-3 is a pro-apoptotic protein. Once cleaved, it is responsible for the majority of proteolysis that occurs during apoptosis. The expression of cleaved caspase-3 was determined here by Western blotting. The results showed

trends for increased levels of cleaved caspase-3 relative to controls following the treatment of KKU-213A and TFK-1 cells with SRPK inhibitors (Fig. 3E,F). Quantification of the protein band intensity revealed that treatment with 20 μ M SPHINX31 significantly increased the level of cleaved caspase-3 expression in TFK-1 cells (Fig. 3F).

3.5 Effect of SRPK Inhibitors on the Phosphorylation of SRSFs in CCA Cells

SRPKs are responsible for the phosphorylation of SRSFs, thereby inducing the nuclear localization of SRSFs and their ability to act as splicing factors. We investigated the effect of SRPK inhibitors on the phosphorylation of SRSF proteins in CCA cells by performing Western blot analysis with an anti-phosphoepitope SR protein antibody. These phosphoepitopes are present in each of the SRSF1-SRSF12 domains, but can be distinguished by differences in the molecular weight (MW) of the various pSRSFs.

The apoptotic cell populations and apoptotic protein activation in TFK-1 cells were investigated following treatment with SRPIN340 and SPHINX31 (Fig. 3B,D,F). Decreased expression of proteins with an approximate MW of 32, 35 and 40 kDa was observed following treatment with 10 μ M and 20 μ M SRPIN340, and with 10 μ M SPHINX31, relative to vehicle controls (Fig. 4A). These protein bands were predicted to be pSRSF1/pSRSF12, pSRSF2/pSRSF7, and pSRSF5/pSRSF10, respectively, according to their MW. SRPIN340 significantly decreased the phosphorylation of pSRSF5/pSRSF10, pSRSF2/pSRSF7 and pSRSF1/pSRSF12 in a dose-dependent manner. Treatment with 10 μ M SPHINX31 significantly decreased the phosphorylation of pSRSF2/pSRSF7 and pSRSF1/pSRSF12, with the trend increasing at 20 μ M SPHINX31 (Fig. 4B).

3.6 Effect of SRPK Inhibitors on the Translocation of SRSF1 from the Cytoplasm to the Nucleus

SRSF1 is the predominant SRSF expressed in various cancer types. Of note, pSRSF1/pSRSF12 was significantly decreased after treatment of TFK-1 cells with SRPK in-

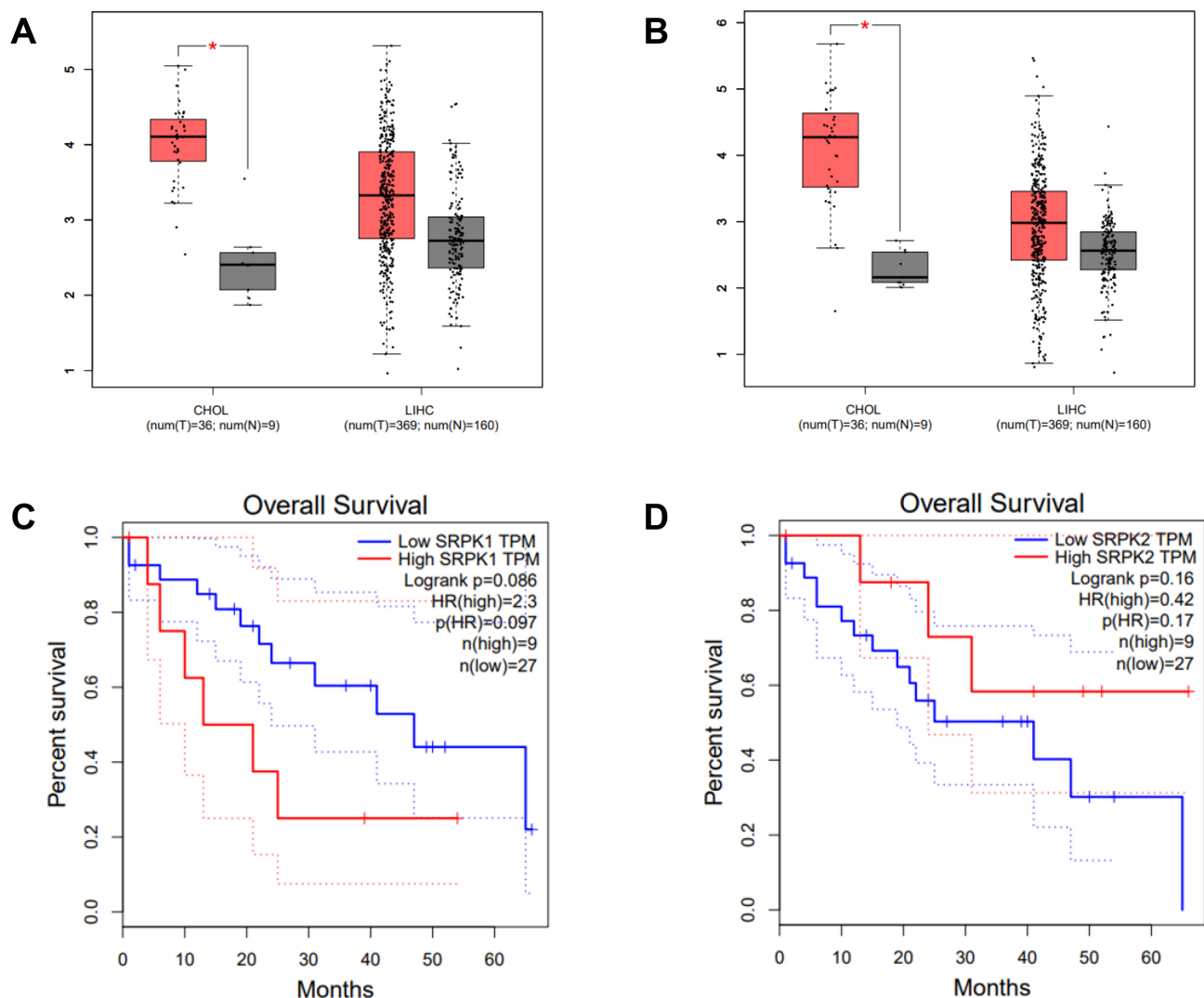


Fig. 1. Expression of *SRPK1* and *SRPK2* (transcripts per million, TPM), and correlation with the survival of CHOL patients (TCGA dataset, GEPIA analysis). Box-plot analysis comparing the expression levels of *SRPK1* (A) and *SRPK2* (B) in the cancer tissue of CHOL and LIHC patients. Tumor tissue (T; red box), normal adjacent tissue (N; grey box). Overall survival of CHOL patients according to high and low expression of *SRPK1* (C), and *SRPK2* (D). High *SRPK1* expression was associated with a significantly worse survival rate (HR = 2.3) (C), whereas high *SRPK2* expression showed no significant association with survival (D). * $p < 0.05$. CHOL, cholangiocarcinoma; LIHC, Liver hepatocellular carcinoma; TCGA, The Cancer Genome Atlas; GEPIA, Gene Expression Profiling Interactive Analysis; SRPK, serine/arginine protein kinase; HR, hazard ratio.

hibitors (Fig. 4A,B). Therefore, a concentration of 20 μ M of SRPK inhibitor was chosen to investigate the translocation of SRSF1 from the cytoplasm to the nucleus. IF and Western blotting were employed to study the effect of SRPK inhibitors on this translocation,

Under fluorescence microscopy, red fluorescence represents the localization of SRSF1 and is merged with DAPI staining to mark the nucleus. SRSF1 was mainly localized in the area with DAPI-marked nuclei in the vehicle control cells, but was dispersed into the cytoplasmic area after treatment with 20 μ M SRPIN340 or SPHINX31 (Fig. 4C). To confirm the cytoplasmic vs. nuclear accumulation of SRSF1, Western blotting of SRSF1 protein was performed

after subcellular protein fractionation. Relative to the vehicle control, higher SRSF1 levels were found in the cytoplasmic fraction and lower levels in the nuclear fraction after treatment with SRPK inhibitor, especially for 20 μ M SPHINX31 (Fig. 4D).

3.7 Effect of SRPK Inhibitors on Alternative mRNA Splicing of Apoptosis-related Genes

After showing that treatment with SRPK inhibitors reduced SRSF phosphorylation (Fig. 4A) and the nuclear translocation of SRSFs (Fig. 4B), we next investigated changes in gene splicing errors. SRPK inhibitor treatment of TFK-1 cells clearly induced apoptosis (Fig. 3B,D,F).

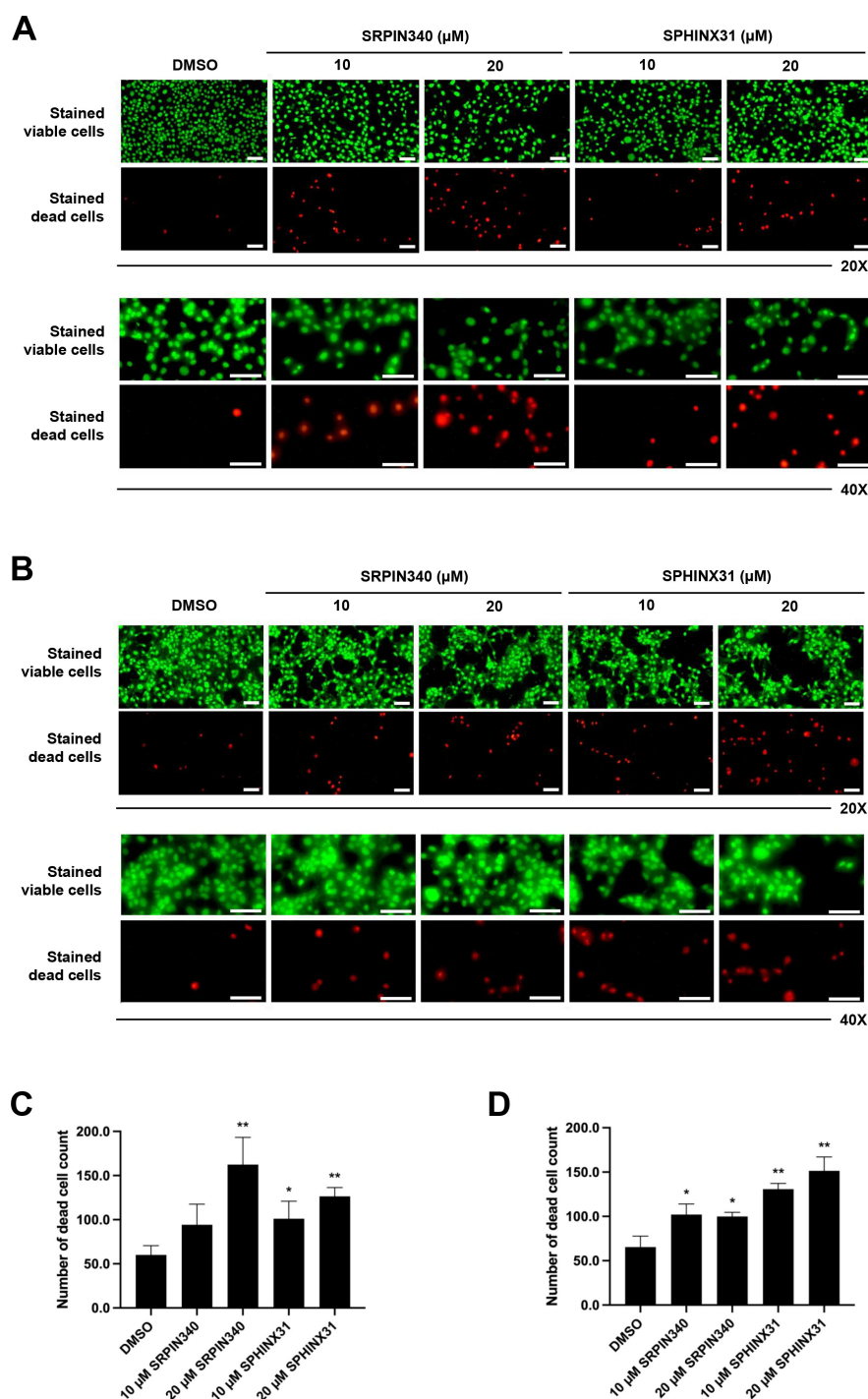


Fig. 2. Effects of SRPIN340 and SPHINX31 on the induction of CCA cell death. Fluorescence microscopy images of live/dead cell dual staining of CCA cells treated with the SRPK inhibitors SRPIN340 and SPHINX31 (20× and 40× magnification). Viable cells stain green fluorescent and dead cells stain red fluorescent. KKU-213A (A), and TFK-1 (B). Counts for red fluorescent cells are shown in the bar graph, with the Y-axis for the dead cell count in KKU-213A (C), and TFK-1 (D) cells. Statistical analysis was performed on data from three independent experiments. Scale bar = 100 μm. * $p < 0.05$ and ** $p < 0.01$. CCA, Cholangiocarcinoma; DMSO, dimethyl sulfoxide.

We therefore investigated splicing errors in the apoptotic-related genes *BIN1*, *MCL1* and *BCL2*. The results showed that treatment with SRPIN340 or SPHINX31 significantly

decreased the level of anti-apoptotic *BIN1+12A*, but not *BIN1* all-forms (Fig. 5A,B), possibly explaining the restoration of cellular apoptosis. Furthermore, the levels of pro-

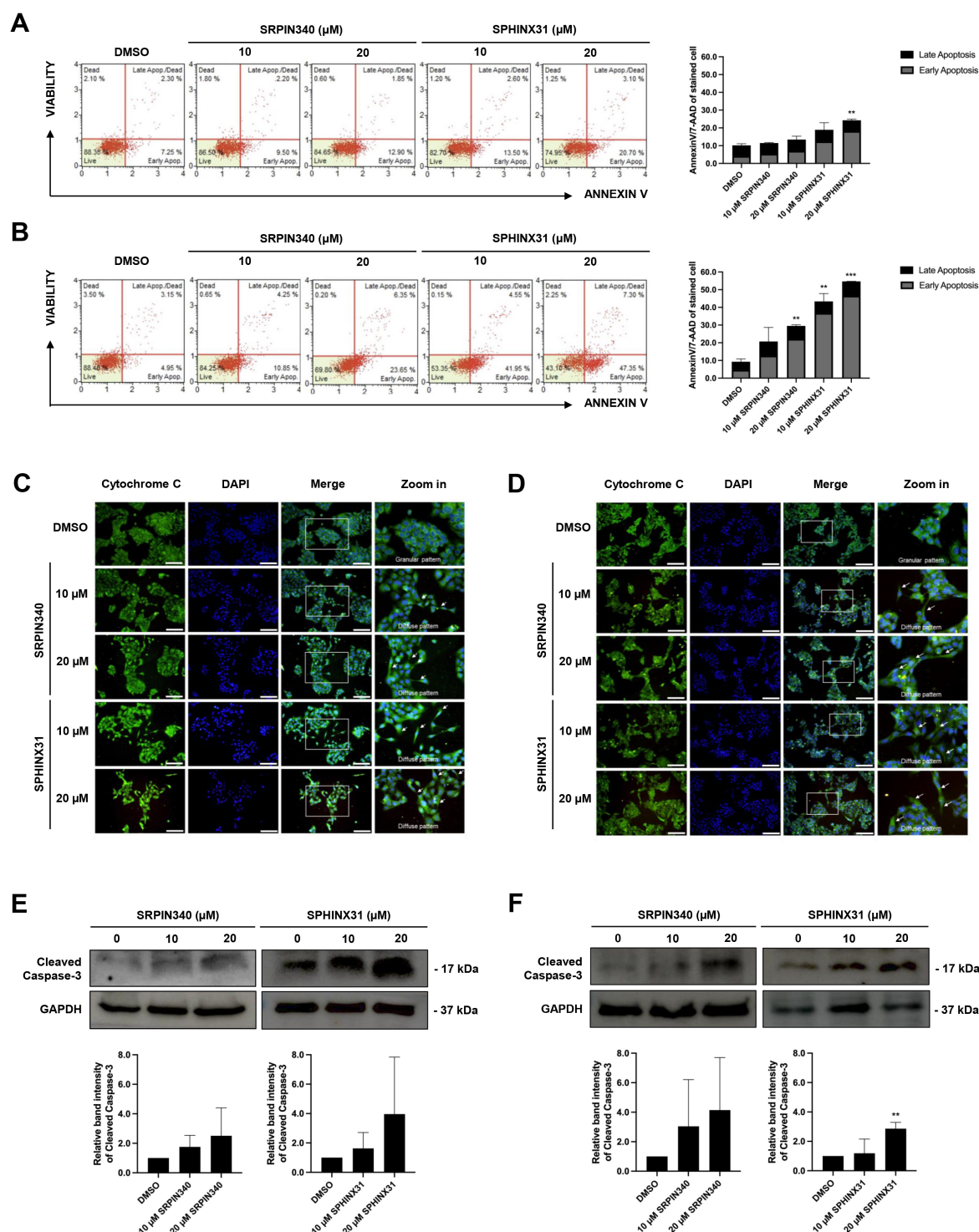


Fig. 3. Effect of SRPIN340 and SPHINX31 on CCA cell apoptosis. AnnexinV/7-AAD staining coupled with flow cytometry was used to gate apoptotic cell populations after SRPIN340 or SPHINX31 treatment of KCU-213A (A) and TFK-1 (B) cells. The percentage of cells in each staining quadrant was calculated and is shown in the bar graph. Early apoptosis is represented as grey color, and late apoptosis as black color. Immunofluorescence (IF) was used to track mitochondrial leakage of cytochrome C, thus allowing the evaluation of apoptotic induction in KCU-213A (C) and TFK-1 (D) cells following treatment with SRPIN340 or SPHINX31. The white arrows indicate the diffuse pattern of cytoplasmic cytochrome C. Western blot analysis of cleaved caspase-3 was performed to assess the induction of caspase-dependent apoptosis in KCU-213A (E) and TFK-1 (F) cells treated with SRPIN340 or SPHINX31. Statistical analysis was performed on data from three independent experiments. Scale bar = 100 μm . $**p < 0.01$, and $***p < 0.001$.

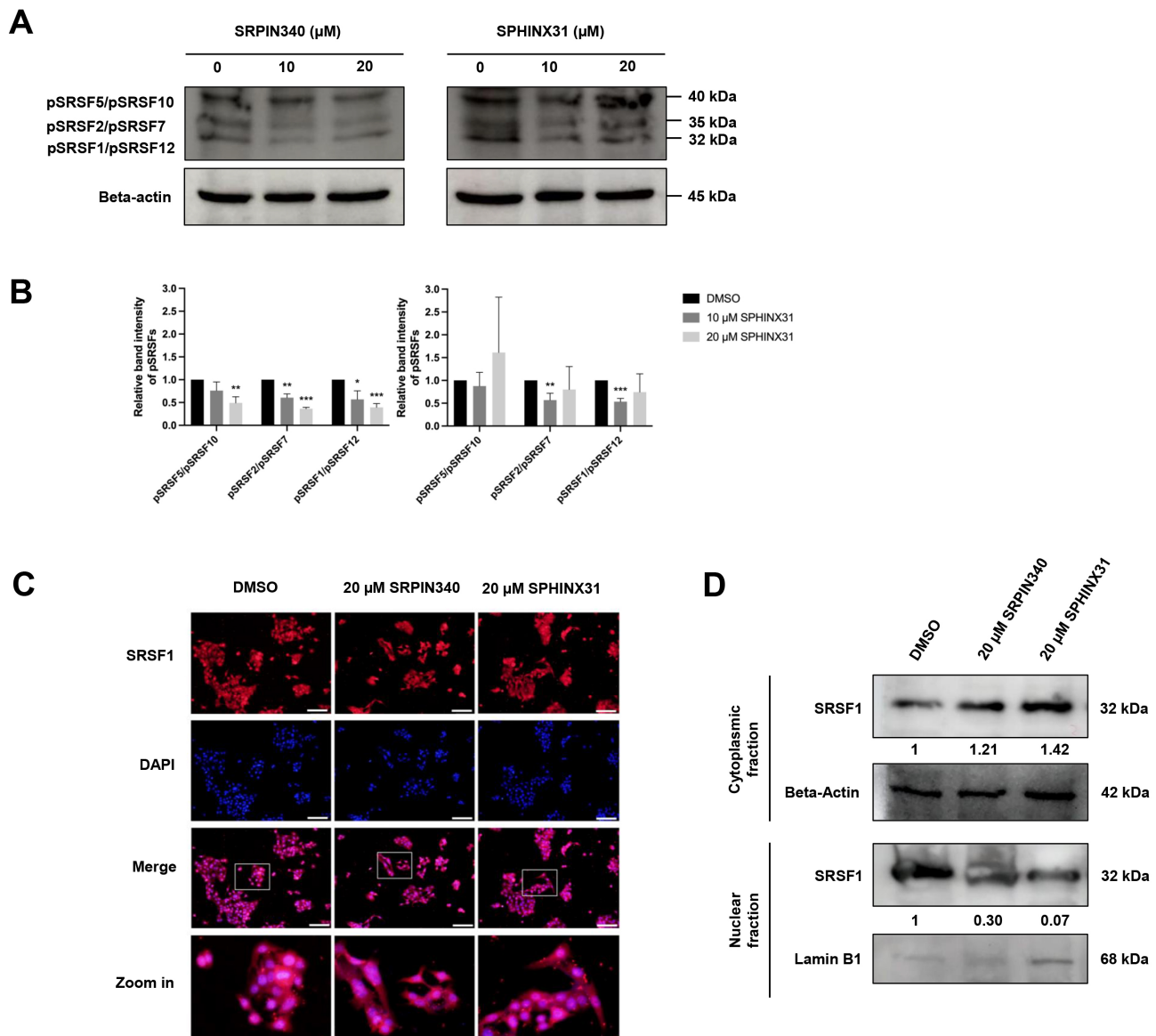


Fig. 4. Inhibitory effects of SRPIN340 and SPHINX31 on the phosphorylation and nuclear translocation of splicing factors in TFK-1 cells. Western blot analysis of SRSFs with anti-phosphoepitope SR protein antibody in TFK-1 cells treated with SRPIN340 or SPHINX31 (A). The band intensity for each phospho-SRSF was calculated and the SRSFs were identified by their predicted molecular weight (B). Immunofluorescence (IF) staining of the predominant SRSF1 is represented as red fluorescence, while the cell nuclei are marked by DAPI staining (C). Western blot analysis of SRSF1 protein derived from cellular fractionation revealed the accumulation of SRSF1 following treatment with SRPK inhibitors (D). Statistical analysis was performed on data from three independent experiments. $*p < 0.05$, $**p < 0.01$, $***p < 0.001$. SRSF, serine/arginine rich-splicing factor; DAPI, 4',6-diamidino-2-phenylindole.

apoptotic *MCL-1S* (Fig. 5C,D) and *BCL-xS* (Fig. 5E,F) isoforms were increased, thus enabling the cellular apoptosis of TFK-1 cells.

4. Discussion

Analysis of the TCGA dataset revealed the level of SRPK1 and SRPK2 transcripts was significantly higher in CCA tumor tissue than in normal adjacent tissue. Moreover, high SRPK1 expression was associated with shorter overall survival of CCA patients. We subsequently used

the SRPK inhibitors SRPIN340 and SPHINX31 for *in vitro* studies with the CCA cell lines KCU-213A and TFK-1. Treatment with these inhibitors induced apoptosis, particularly in TFK-1 cells. Consequently, phosphorylation of the splicing factors was blocked, resulting in the cytoplasmic accumulation of the predominant splicing factor SRSF1. Lastly, the correction of splicing errors could be explained by decreased levels of *BINI+12A* and increased levels of *MCL-1S* and *BCL-xS*, which were recovered by treatment with SRPK inhibitor.

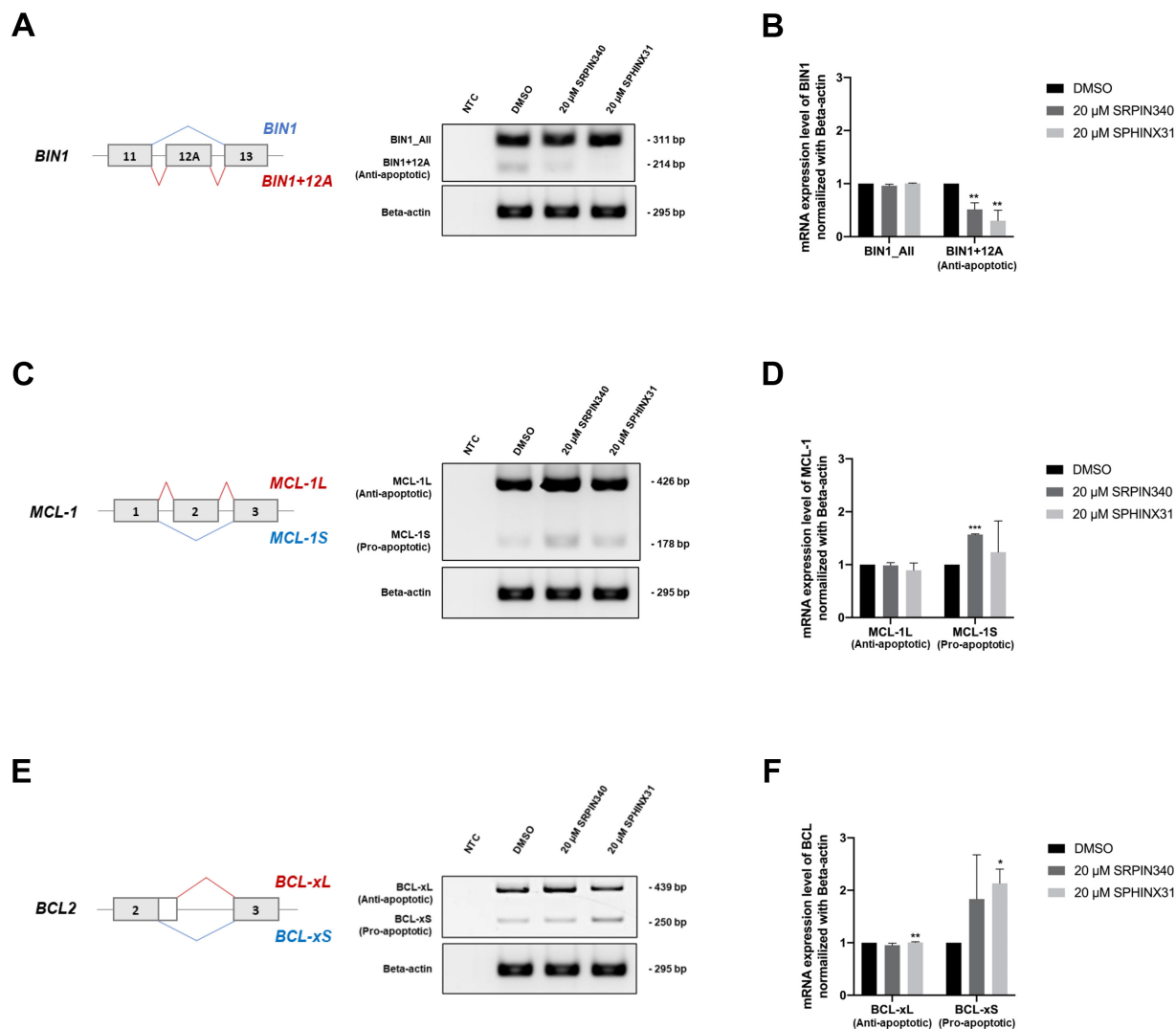


Fig. 5. Effect of SRPIN340 and SPHINX31 on the correction of splicing errors in apoptosis-related genes in TFK-1 cells. Reverse transcription-polymerase chain reaction (RT-PCR) was performed to quantify splicing of the apoptosis-related genes *BIN1*, *MCL1* and *BCL2*. The level of the anti-apoptotic *BIN1+12A* isoform was compared to that of *BIN1_All*, comprising all isoforms (A), with the normalized intensity shown in the bar graph (B). The level of pro-apoptotic *MCL-1S* was also compared to that of *MCL-1L* (C), with the normalized intensity shown in the bar graph (D). The level of pro-apoptotic *BCL-xS* was compared to that of *BCL-xL* (E), with the normalized intensity shown in the bar graph (F). Statistical analysis was performed on data from three independent experiments. * $p < 0.05$, ** $p < 0.01$, and *** $p < 0.001$. NTC, No template control.

Aberrant alternative splicing has been recognized as part of the oncogenic machinery during the development of cancer. SRSFs are part of the SR protein family and are key molecules regulated by SRPKs [19,27]. Several studies have established the contribution of specific SRPKs in cancers. Elevated expression of SRPK1 enhances the anti-apoptosis capacity of colon cancer cells through the SRPK1/AKT axis and NF- κ B activation, whereas the silencing of SRPK1 expression induced apoptosis [28]. Moreover, silencing of SRPK1 expression by specific-

siRNA induced apoptosis of the myelogenous leukemia cell line K562 via the PARP-caspase-3 pathway [29]. In addition, knockdown of SRPK1 in the esophageal squamous cell carcinoma cell line EC109 increased the number of TUNEL-positive cells and the activation of caspase-3 [30]. Finally, the silencing of SRPK1 expression by specific-siRNA resulted in decreased cell growth and migration, significantly increased apoptosis, and reduced angiogenesis in human colorectal cancer cells [31].

We studied the dysregulation of SRSFs and SRPKs leading to aberrant mRNA and protein synthesis and contributing to the oncogenesis of CCA [7]. Many studies in various cancer types have reported that overexpression of SRPK1 and SRPK2 correlated with advanced tumor stage and poor prognosis [32]. The SRPK inhibitor SRPIN340 demonstrated inhibitory effects on both SRPK1 and SRPK2 [33], whereas SPHINX31 was shown to inhibit SRPK1 only [34].

The present study showed that SRPIN340 and SPHINX31 significantly increased cell death in the KLU-213A and TFK-1 cell lines (Fig. 2), thus confirming previous reports that SPHINX31 decreased the growth of leukemic cells [35], and in xenografted-prostate cancer cells [36]. Interestingly, SPHINX31 significantly reduced the Ki-67 for proliferation suppression of umbilical vein endothelial cells (HUVECs) [37]. We found that SRPIN340 and SPHINX31 treatment of CCA cells increased the early apoptotic population in a dose-dependent manner, especially in TFK-1 cells (Fig. 3A,B). A previous study in lymphoma found that SPHINX31 and SRPIN340 increased ENKTL-related cell apoptosis [20]. SRPIN340 can also trigger early and late apoptosis in leukemia cells [21]. Moreover, depletion of SRPK1 by siRNA or shRNA increased the apoptosis of pancreatic carcinoma and glioma cells [38–40]. We also showed that SPHINX31 and SRPIN340 caused mitochondrial leakage of cytochrome C and increased the level of the cleaved form of caspase-3 protein (Fig. 3C–F). These observations are similar to previous results on endometrial cancer in which SPHINX31 reduced survivin expression and increased the level of cleaved PARP to induce apoptosis of SPEC-2 cells [22]. In addition, SRPIN340 and SPHINX31 increased the levels of cleaved PARP and cleaved caspase-3 in ENKTL cells [20].

SRPKs are responsible for the phosphorylation of splicing factors. The present study found lower levels of SRSF phosphorylation following treatment of TFK-1 cells with SRPK inhibitors (Fig. 4A,B). Interestingly, treatment with SPHINX31 resulted in non-linear changes in SRSF phosphorylation levels. A previous study on leukemic cancer cells (HL60 and Jurkat cells) suggested the optimal period to measure SRSF phosphorylation was 18 h after treatment rather than 9 h [21]. An intracellular feedback mechanism may occur under high dose treatment. HuCCA-1 cells also showed non-linear changes in the phosphorylation level at various inhibitor concentrations, with similar intensities of phospho-SRSF1 observed from 0.3–10 μ M of SPHINX31 [23]. The dephosphorylation effect of SRPK inhibitors has been validated in several cancer cell models. SRPIN340 decreased the phosphorylation of SRSF2, SRSF4, SRSF5 and SRSF6 in HL60 and Jurkat cells [21], SPHINX31 decreased the kinase activity of SRPK1 by reducing the phosphorylated form of SRSFs in SPEC-2 cells [22], SPHINX31 reduced SRSF1 phosphorylation in RPE cells [34]. In addition, treatment by SRPIN340 and

SPHINX31 reduced the EGF-dependent phosphorylation of SRSF1 and SRSF2 in PC-3 prostate cancer cells [36]. An earlier study on CCA cells showed that SPHINX31 reduced SRSF1 phosphorylation in HuCCA-1 cells [23]. Apart from SRPIN340 and SPHINX31, a docking blocker of SRPK1 (DBS1) inhibits protein-protein interactions of SRPKs, thus effectively preventing the phosphorylation of SRSF1 in A375 and HeLa cells [41]. We tracked the nuclear translocation of SRSF1, which is the predominantly expressed SRSF in cancer. We found that SRSF1 accumulated in the cytoplasm of TFK-1 cells following treatment with SRPK inhibitors (Fig. 4C,D). Similar results have been reported in other cancer types, with SRPIN340 effectively reducing SRPK1 nuclear translocation and phosphorylation of SR proteins in the murine melanoma cell line B16F10 [42].

Treatment with SRPK inhibitor reduced SRSF1 phosphorylation and its cytoplasmic accumulation. Lower SRSF phosphorylation and cytoplasmic accumulation of SRSF1 were associated with CCA cell death and were subsequently explained by the splicing of SRSF1-targeted mRNA. Three genes that contain SRSF1 recognition sequences (GAAGAA and (A/G)GAAGAAC) and which contribute to cancer cell apoptosis were selected for further study. We confirmed the correction of gene-splicing errors by SRPK inhibitors in the apoptosis-related genes *BIN1*, *MCL-1* and *BCL*. Alignment analysis of the SRSF1 recognition sequences with the full-length mRNA of each gene revealed three recognition sites within *BIN1* mRNA (exons 1, 6 and 10), two within *MCL-1* mRNA (exon 3), and 6 within *BCL* mRNA (exon 3). Decreased *BIN1+12A* and increased *MCL-1S* and *BCL-xS* were associated with the induction of apoptosis in TFK-1 cells (Fig. 5A–C). Similar results have been reported for other treatments or agents in various cancer types. For example, aberrant splicing of *BIN1* to *BIN1+12A* attenuated cell death mediated by E2F1 and etoposide, independently of the p53- and p73-mediated pathways, leading to DNA damage-induced cell death [9]. Moreover, *BIN1+12A* was shown to be under the control of SRSF1 in non-small cell lung cancer (NSCLC). *BIN1+12A* exerts anti-apoptotic properties in NSCLC through changes in its subcellular localization [11]. With *MCL-1* splicing, *Mcl-1S* overexpression induced apoptosis in basal cell carcinoma (BCC) cells. Antisense morpholino oligonucleotides (AMOs) for *MCL-1* can specifically target *MCL-1* pre-mRNA and shift the splicing pattern from *MCL-1L* to *MCL-1S* mRNA and protein. This shift induces apoptosis in BCC cells, as shown by the increased population of sub-G1 apoptotic cells in *MCL-1S*-transfected cells [12]. In addition, the modification of *MCL-1* splicing in gastric cancer cells stimulates pro-apoptotic factors, including cleaved-caspase-9, BAK and cleaved caspase-3 [43]. Finally, dysregulation of alternative splicing for the *BCL* gene promoted the upregulation of *BCL-xS* in pancreatic β -cells, resulting in apoptosis via the suppression of *BCL-xL*. BAX

and BAK were then activated to promote cytochrome C leakage and activation of caspase-3 [44]. Evidence for the role of SRPK inhibitors in the correction of gene splicing has only been obtained for *VEGF*. SPHINX31 decreased the pro-angiogenic *VEGF-A165a* isoform and increased the ratio of VEGF-A165b/total VEGF-A protein to attenuate angiogenesis [12].

5. Conclusions

The contribution of aberrant alternative mRNA splicing in cancer development and progression is well recognized, particularly in CCA. There is now considerable evidence documenting the overexpression, overactivation, or dysregulation of splicing factor SRSFs as a consequence of uncontrolled phosphorylation by splicing kinase SRPKs. Upregulation of *SRPK1* and *SRPK2* in CCA was observed following analysis of the TCGA dataset. This study explored the cellular effects of the potent SRPK inhibitors SRPIN340 and SPHINX31 in CCA cells. Two CCA cell lines representing iCCA (KKU-213A) and eCCA (TFK-1) were treated with SRPK inhibitors to investigate their ability to induce cell death. The number of dead and apoptotic cell populations were increased after treatment and were characterized by the apoptosis-related proteins cytochrome C and cleaved caspase-3. Moreover, reduced SRSF phosphorylation and nuclear translocation were observed after treatment with the inhibitors, especially for SRSF1. Finally, additional insight into the downstream regulation and correction of splicing errors in apoptosis-related genes was obtained. Reduced levels of anti-apoptotic *BIN1+12A*, and increased levels of pro-apoptotic *MCL-1S* and *BCL-xS* could explain the induction of apoptosis in CCA cells following treatment with SRPK inhibitors. This study may serve as a basis for the targeting of SRPKs as an alternative treatment strategy for CCA.

Abbreviations

AGR2, Anterior gradient-2; *BCC*, Basal cell carcinoma; *BCL-2*, B-cell lymphoma 2; *BIN1*, Bridging Integrator 1; *CCA/CHOL*, Cholangiocarcinoma; *CD44*, Cluster of Differentiation; *c-MYC*, Cellular myelocytomatosis oncogene; *DMSO*, dimethyl sulfoxide; *eCCA*, extrahepatic cholangiocarcinoma; *ENKTL*, extranodal NK/T-cell lymphoma; *GEPIA*, Gene Expression Profiling Interactive Analysis; *GTEX*, Genotype-Tissue Expression; *HR*, Hazard ratio; *iCCA*, intrahepatic cholangiocarcinoma; *IF*, Immunofluorescence; *LIHC*, liver hepatocellular carcinoma; *MCL-1*, Myeloid cell leukemia factor 1; *NTC*, No template control; *OV*, *Opisthorchis viverrini*; *PARP*, Poly-Adenosine diphosphate ribose polymerase; *pSRSFs*, phospho-SRSFs; *RT-PCR*, Reverse Transcription-Polymerase Chain Reaction; *SRPKs*, serine-arginine protein kinases; *SRSFs*, serine/arginine rich-splicing factors; *STR*, Short Tandem Repeat; *TCGA*, The Cancer Genome

Atlas; *TPM*, Transcript per million; *VEGF*, vascular endothelial growth factor; *WB*, Western blotting; *WISP1*, Wnt-Inducible Secreted Protein 1.

Availability of Data and Materials

The data presented in this study are available upon request from corresponding author.

Author Contributions

PC, TJ, WK conceived and designed the work; WK, SH, SK, SP, DS curated data; PC, CI performed the experiments; PC, CI, AS, WK analyzed the data; PC, CI, WK wrote the manuscript; SP, DS, TJ, WK administrated project; SK, AS, TJ, WK supervised. All authors contributed to editorial changes in the manuscript. All authors read and approved the final manuscript. All authors have participated sufficiently in the work and agreed to be accountable for all aspects of the work.

Ethics Approval and Consent to Participate

The KKU-213A cell line was established from a 58-year-old male diagnosed with iCCA at the Srinagarind Hospital, Khon Kaen University, Thailand, which the patients' informed consent and the research protocol (HE621403) was formerly approved by the Ethics Committee for Human Research of Khon Kaen University.

Acknowledgment

Not applicable.

Funding

This study was supported by the grant from National Research Council of Thailand, NRCT-Research Career Development Grant (NRCT5-RSA63011-04).

Conflict of Interest

The authors declare no conflict of interest.

References

- [1] Kodali S, Shetty A, Shekhar S, Victor DW, Ghobrial RM. Management of Intrahepatic Cholangiocarcinoma. *Journal of Clinical Medicine*. 2021; 10: 2368.
- [2] Banales JM, Marin JJG, Lamarca A, Rodrigues PM, Khan SA, Roberts LR, *et al.* Cholangiocarcinoma 2020: the next horizon in mechanisms and management. *Nature Reviews. Gastroenterology & Hepatology*. 2020; 17: 557–588.
- [3] Young ND, Nagarajan N, Lin SJ, Korhonen PK, Jex AR, Hall RS, *et al.* The *Opisthorchis viverrini* genome provides insights into life in the bile duct. *Nature Communications*. 2014; 5: 4378.
- [4] Prueksapanich P, Piyachaturawat P, Aumpansub P, Rittitid W, Chaiteerakij R, Rerknimitr R. Liver Fluke-Associated Biliary Tract Cancer. *Gut and Liver*. 2018; 12: 236–245.
- [5] Lodomery M. Aberrant alternative splicing is another hallmark of cancer. *International Journal of Cell Biology*. 2013; 2013: 463786.
- [6] Fackenthal JD, Godley LA. Aberrant RNA splicing and its func-

- tional consequences in cancer cells. *Disease Models & Mechanisms*. 2008; 1: 37–42.
- [7] Yosudjai J, Wongkham S, Jirawatnotai S, Kaewkong W. Aberrant mRNA splicing generates oncogenic RNA isoforms and contributes to the development and progression of cholangiocarcinoma. *Biomedical Reports*. 2019; 10: 147–155.
 - [8] Suwanmanee G, Yosudjai J, Phimsen S, Wongkham S, Jirawatnotai S, Kaewkong W. Upregulation of AGR2vH facilitates cholangiocarcinoma cell survival under endoplasmic reticulum stress via the activation of the unfolded protein response pathway. *International Journal of Molecular Medicine*. 2020; 45: 669–677.
 - [9] Ge K, DuHadaway J, Du W, Herlyn M, Rodeck U, Prendergast GC. Mechanism for elimination of a tumor suppressor: aberrant splicing of a brain-specific exon causes loss of function of Bin1 in melanoma. *Proceedings of the National Academy of Sciences of the United States of America*. 1999; 96: 9689–9694.
 - [10] Folk WP, Kumari A, Iwasaki T, Pyndiah S, Johnson JC, Casimere EK, *et al.* Loss of the tumor suppressor BIN1 enables ATM Ser/Thr kinase activation by the nuclear protein E2F1 and renders cancer cells resistant to cisplatin. *The Journal of Biological Chemistry*. 2019; 294: 5700–5719.
 - [11] Wang J, Liu T, Wang M, Lv W, Wang Y, Jia Y, *et al.* SRSF1-dependent alternative splicing attenuates BIN1 expression in non-small cell lung cancer. *Journal of Cellular Biochemistry*. 2020; 121: 946–953.
 - [12] Shieh JJ, Liu KT, Huang SW, Chen YJ, Hsieh TY. Modification of alternative splicing of Mcl-1 pre-mRNA using antisense morpholino oligonucleotides induces apoptosis in basal cell carcinoma cells. *The Journal of Investigative Dermatology*. 2009; 129: 2497–2506.
 - [13] Gautrey HL, Tyson-Capper AJ. Regulation of Mcl-1 by SRSF1 and SRSF5 in cancer cells. *PloS One*. 2012; 7: e51497.
 - [14] Larrayoz M, Blakemore SJ, Dobson RC, Blunt MD, Rose-Zerilli MJJ, Walewska R, *et al.* The SF3B1 inhibitor spliceostatin A (SSA) elicits apoptosis in chronic lymphocytic leukaemia cells through downregulation of Mcl-1. *Leukemia*. 2016; 30: 351–360.
 - [15] Massiello A, Roesser JR, Chalfant CE. SAP155 Binds to ceramide-responsive RNA cis-element 1 and regulates the alternative 5' splice site selection of Bcl-x pre-mRNA. *FASEB Journal: Official Publication of the Federation of American Societies for Experimental Biology*. 2006; 20: 1680–1682.
 - [16] Hossini AM, Geilen CC, Fecker LF, Daniel PT, Eberle J. A novel Bcl-x splice product, Bcl-xAK, triggers apoptosis in human melanoma cells without BH3 domain. *Oncogene*. 2006; 25: 2160–2169.
 - [17] Choi S, Chen Z, Tang LH, Fang Y, Shin SJ, Panarelli NC, *et al.* Bcl-xL promotes metastasis independent of its anti-apoptotic activity. *Nature Communications*. 2016; 7: 10384.
 - [18] Änkö ML. Regulation of gene expression programmes by serine-arginine rich splicing factors. *Seminars in Cell & Developmental Biology*. 2014; 32: 11–21.
 - [19] Giannakouros T, Nikolakaki E, Mylonis I, Georgatsou E. Serine-arginine protein kinases: a small protein kinase family with a large cellular presence. *The FEBS Journal*. 2011; 278: 570–586.
 - [20] He C, Liu B, Wang HY, Wu L, Zhao G, Huang C, *et al.* Inhibition of SRPK1, a key splicing regulator, exhibits antitumor and chemotherapeutic-sensitizing effects on extranodal NK/T-cell lymphoma cells. *BMC Cancer*. 2022; 22: 1100.
 - [21] Siqueira RP, Barbosa ÉDAA, Polêto MD, Righetto GL, Seraphim TV, Salgado RL, *et al.* Potential Antileukemia Effect and Structural Analyses of SRPK Inhibition by N-(2-(Piperidin-1-yl)-5-(Trifluoromethyl)Phenyl)Isonicotinamide (SRPIN340). *PloS One*. 2015; 10: e0134882.
 - [22] Kurimchak AM, Kumar V, Herrera-Montávez C, Johnson KJ, Srivastava N, Davarajan K, *et al.* Kinome Profiling of Primary Endometrial Tumors Using Multiplexed Inhibitor Beads and Mass Spectrometry Identifies SRPK1 as Candidate Therapeutic Target. *Molecular & Cellular Proteomics: MCP*. 2020; 19: 2068–2090.
 - [23] Supradit K, Boonsri B, Duangdara J, Thitiphatphuvanon T, Suriyonplengsaeng C, Kangsamaksin T, *et al.* Inhibition of serine/arginine-rich protein kinase-1 (SRPK1) prevents cholangiocarcinoma cells induced angiogenesis. *Toxicology in Vitro: an International Journal Published in Association with BIBRA*. 2022; 82: 105385.
 - [24] Sripa B, Seubwai W, Vaeteewoottacharn K, Sawanyawisuth K, Silsirivanit A, Kaewkong W, *et al.* Functional and genetic characterization of three cell lines derived from a single tumor of an Opisthorchis viverrini-associated cholangiocarcinoma patient. *Human Cell*. 2020; 33: 695–708.
 - [25] Saijo S, Kudo T, Suzuki M, Katayose Y, Shinoda M, Muto T, *et al.* Establishment of a new extrahepatic bile duct carcinoma cell line, TFK-1. *The Tohoku Journal of Experimental Medicine*. 1995; 177: 61–71.
 - [26] Andrews NC, Faller DV. A rapid micropreparation technique for extraction of DNA-binding proteins from limiting numbers of mammalian cells. *Nucleic acids research*. 1991; 19: 2499.
 - [27] Änkö ML, Müller-McNicoll M, Brandl H, Curk T, Gorup C, Henry I, *et al.* The RNA-binding landscapes of two SR proteins reveal unique functions and binding to diverse RNA classes. *Genome Biology*. 2012; 13: R17.
 - [28] Huang JQ, Li HF, Zhu J, Song JW, Zhang XB, Gong P, *et al.* SRPK1/AKT axis promotes oxaliplatin-induced anti-apoptosis via NF-κB activation in colon cancer. *Journal of Translational Medicine*. 2021; 19: 280.
 - [29] Wang H, Ge W, Jiang W, Li D, Ju X. SRPK1 siRNA suppresses K562 cell growth and induces apoptosis via the PARP caspase3 pathway. *Molecular Medicine Reports*. 2018; 17: 2070–2076.
 - [30] Ren G, Sheng L, Liu H, Sun Y, An Y, Li Y. The crucial role of SRPK1 in TGF-β-induced proliferation and apoptosis in the esophageal squamous cell carcinomas. *Medical Oncology (Northwood, London, England)*. 2015; 32: 209.
 - [31] Yi N, Xiao M, Jiang F, Liu Z, Ni W, Lu C, *et al.* SRPK1 is a poor prognostic indicator and a novel potential therapeutic target for human colorectal cancer. *OncoTargets and Therapy*. 2018; 11: 5359–5370.
 - [32] Nikas IP, Themistocleous SC, Paschou SA, Tsamis KI, Ryu HS. Serine-Arginine Protein Kinase 1 (SRPK1) as a Prognostic Factor and Potential Therapeutic Target in Cancer: Current Evidence and Future Perspectives. *Cells*. 2019; 9: 19.
 - [33] Fukuhara T, Hosoya T, Shimizu S, Sumi K, Oshiro T, Yoshinaka Y, *et al.* Utilization of host SR protein kinases and RNA-splicing machinery during viral replication. *Proceedings of the National Academy of Sciences of the United States of America*. 2006; 103: 11329–11333.
 - [34] Batson J, Toop HD, Redondo C, Babaei-Jadidi R, Chaikuad A, Wearmouth SF, *et al.* Development of Potent, Selective SRPK1 Inhibitors as Potential Topical Therapeutics for Neovascular Eye Disease. *ACS Chemical Biology*. 2017; 12: 825–832.
 - [35] Tzelepis K, De Braekeleer E, Aspris D, Barbieri I, Vijayabaskar MS, Liu WH, *et al.* SRPK1 maintains acute myeloid leukemia through effects on isoform usage of epigenetic regulators including BRD4. *Nature Communications*. 2018; 9: 5378.
 - [36] Mavrou A, Brakspear K, Hamdollah-Zadeh M, Damodaran G, Babaei-Jadidi R, Oxley J, *et al.* Serine-arginine protein kinase 1 (SRPK1) inhibition as a potential novel targeted therapeutic strategy in prostate cancer. *Oncogene*. 2015; 34: 4311–4319.
 - [37] Gu YY, Tan XH, Song WP, Song WD, Yuan YM, Xin ZC, *et al.* Icariside II Attenuates Palmitic Acid-Induced Endothelial Dysfunction Through SRPK1-Akt-eNOS Signaling Pathway. *Front*

- tiers in Pharmacology. 2022; 13: 920601.
- [38] Hayes GM, Carrigan PE, Beck AM, Miller LJ. Targeting the RNA splicing machinery as a novel treatment strategy for pancreatic carcinoma. *Cancer Research*. 2006; 66: 3819–3827.
 - [39] Chang Y, Wu Q, Tian T, Li L, Guo X, Feng Z, *et al*. The influence of SRPK1 on glioma apoptosis, metastasis, and angiogenesis through the PI3K/Akt signaling pathway under normoxia. *Tumour Biology: the Journal of the International Society for Oncodevelopmental Biology and Medicine*. 2015; 36: 6083–6093.
 - [40] Shi M, Sun D, Deng L, Liu J, Zhang MJ. SRPK1 Promotes Glioma Proliferation, Migration, and Invasion through Activation of Wnt/ β -Catenin and JAK-2/STAT-3 Signaling Pathways. *Biomedicines*. 2024; 12: 378.
 - [41] Li Q, Zeng C, Liu H, Yung K W Y, Chen C, Xie Q, *et al*. Protein-Protein Interaction Inhibitor of SRPKs Alters the Splicing Isoforms of VEGF and Inhibits Angiogenesis. *iScience*. 2021; 24: 102423.
 - [42] Moreira GA, Lima GDDA, Siqueira RP, Barros MVDA, Adjanooun ALM, Santos VC, *et al*. Antimetastatic effect of the pharmacological inhibition of serine/arginine-rich protein kinases (SRPK) in murine melanoma. *Toxicology and Applied Pharmacology*. 2018; 356: 214–223.
 - [43] Li Y, Gao X, Wei C, Guo R, Xu H, Bai Z, *et al*. Modification of Mcl-1 alternative splicing induces apoptosis and suppresses tumor proliferation in gastric cancer. *Aging*. 2020; 12: 19293–19315.
 - [44] Stevens M, Oltean S. Modulation of the Apoptosis Gene Bcl-x Function Through Alternative Splicing. *Frontiers in Genetics*. 2019; 10: 804.